



Short notes on electromagnetic acoustic transducers (EMATs) design and modeling

Hocine Menana ^{a *}, Bruno Douine ^a

^a GREEN, Université de Lorraine, 54506 Vandœuvre-lès-Nancy, France

ARTICLE INFO

Article history :

Received October 2016

Accepted January 2017

Keywords :

EMATs ;
Design ;
Modeling.

ABSTRACT

This paper gives short notes on the electromagnetic acoustic transducers (EMATs) design and modeling. The principle of the electromagnetic-acoustic transduction as well as the various EMATs structures are described, highlighting the important characteristics of each structure. Analytical models are given in global quantities in order to quantify the electromagnetic-acoustic transduction efficiency. The numerical modeling of such structures is also addressed.

©2017 LESI. All rights reserved.

1. Introduction

Electromagnetic acoustic transducers (EMATs) are intended for acoustic wave generation and sensing in conductive material without physical contact, mainly for applications related to material characterization and non-destructive testing (NDT). They are advantageous in situations such as the material to be studied is fragile, moving, heated to a very high temperature, or containing impurities to the surface. Moreover, EMATs offer the ability to control the direction and polarization of the acoustic wave by a simple action on their configuration or their supply. Despite their advantages, EMATs were granted little interest for years due to their relatively low signal to noise ratio compared to classical acoustic transducers. However, the advances achieved in electronics and in signal processing make EMATs to be interesting alternatives for material control and characterization, and even for energy transfer and data communication. They arouse growing interest among the scientific community, concerning their design [1-8], modelling [9-14] and applications [15-21]. In this context, this paper gives short notes on EMATs design and modeling. Different structures of EMATs are described highlighting some influent parameters on the electromagnetic acoustic transduction.

The next section deals with the EMATs operation principle. Different EMATs structures and characteristics are described in the following sections. The last section addresses the

*Email : hocine.menana@univ-lorraine.fr

numerical modelling of EMATs.

2. EMAT operation

An EMAT is constituted of a high frequency (HF) inductor and a permanent magnet or an electromagnet creating a static magnetic field. Most EMATs operate via Lorentz forces (F) resulting from the interaction between eddy currents (J) created by the HF inductor in the tested material and the magnetostatic field density (B) created by the permanent magnet or electromagnet (Fig. 1).

$$\vec{F} = \vec{J} \times \vec{B} \quad (1)$$

The eddy currents, and thus the Lorentz forces, are created in the skin depth, depending on the magnetic permeability and the electrical conductivity of the tested material, and the operating frequency of the HF inductor. It generally varies from 0.05 to 0.5mm in the MHz range [3]. When the tested material is ferromagnetic, magnetostrictive forces are also created in the tested material. Some types of EMATs use essentially magnetostrictive forces [5, 11].

For the reception, the interaction between an acoustic wave and the magnetostatic induction of the EMAT generates eddy currents in the tested material which can be expressed as follows, where is the acoustic wave velocity [12] :

$$\vec{J} = \sigma \vec{v} \times \vec{B} \quad (2)$$

The magnetic field associated to these eddy currents induces a voltage in a sensing coil which can be the same coil used for the emission.

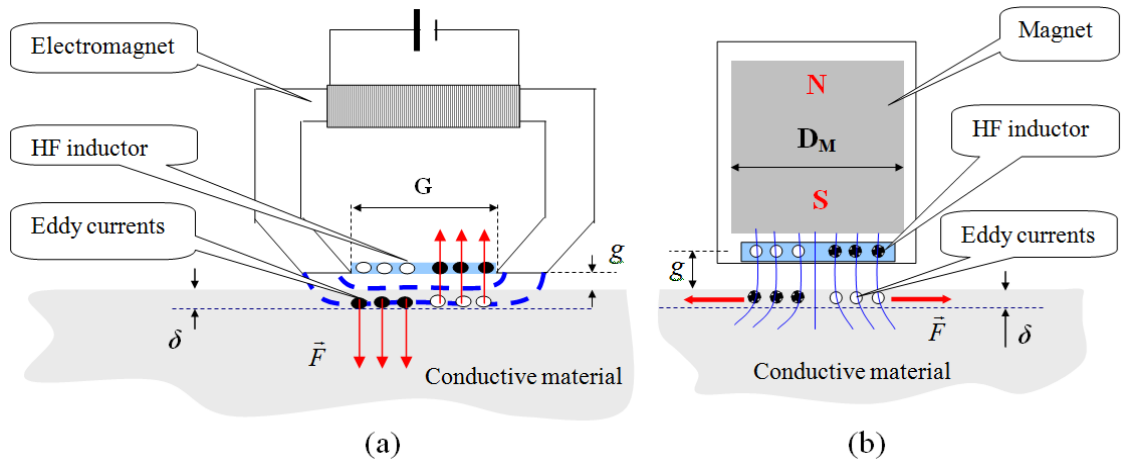


Fig. 1 – EMATs for : (a) longitudinal and (b) transverse waves.

3. EMATs configurations

Figure 1 shows two configurations of EMATs. The configuration that directs the magnetostatic induction parallel to the surface of the material gives rise to longitudinal

(compression) waves (Fig. 1-a), and the configuration that directs the magnetostatic induction perpendicular to the material surface gives rise to transverse waves (Fig. 1-b).

Figure 2 shows the commonly used HF inductors. The spiral coil (fig. 2-a) is very effective for generating radially polarized shear waves [6]. The disadvantage of this coil is that it does not generate pure transverse waves. The ratio between the amplitudes of the transverse and the longitudinal parts of the generated waves is given by (3) [3], where R_S is the spiral coil radius and D_M is the magnet diameter (Fig. 1-b).

$$R_{(\perp - //)} = 0.5 (R_S / D_M)^2 \quad (3)$$

The double spiral coil (Fig. 2-b) is used for longitudinal waves. The serpentine (meander line) coil (Fig. 2-c) allows controlling the orientation of the generated acoustic wave by acting on the supply frequency or on the width of its spatial period. The relation between the surface acoustic waves velocity (v), the supply frequency (f) and the spatial period of the serpentine ($2d$) is given by (4), where θ is the angle between the vector normal to the material surface and the direction of the acoustic wave [16-17].

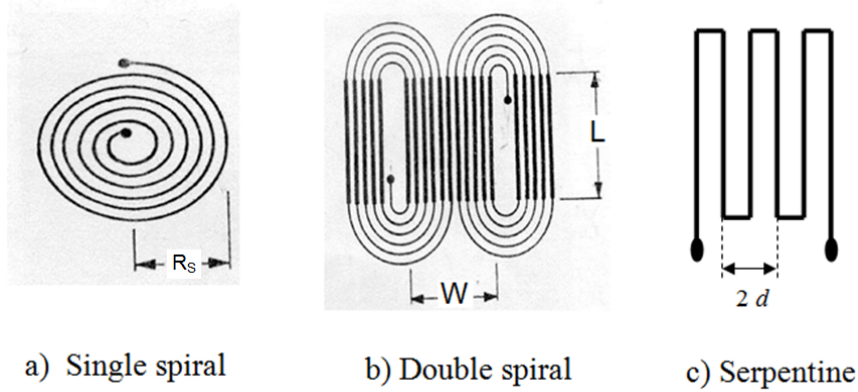


Fig. 2 – The commonly used inductors.

$$\sin \theta = \frac{v}{2df} \quad (4)$$

By choosing appropriate frequency or appropriate spatial period of the serpentine, surface waves ($\theta = \pi/2$) can be generated. For thin plates, the surface waves can be transformed into plate waves when the distance (d) between the serpentine wires is greater than the material thickness [3]. Notice that, according to (4), the acoustic wave cannot be oriented in the direction normal to the surface ($\theta = 0$).

The directivity factor $D(\theta)$ of a serpentine coil is given as follows [4, 7] :

$$D(\theta) = \frac{\sin \left(N \frac{\psi(\theta)}{2} \right)}{N \sin \left(\frac{\psi(\theta)}{2} \right)} e^{j(N-1) \frac{\psi(\theta)}{2}} \quad (5)$$

$$\psi(\theta) = \frac{\omega}{v} d \sin(\theta) + \phi \quad (6)$$

In (5) and (6), N is the number of the coil conductors, ω is the angular frequency and φ is the electrical phase difference between the currents passing through two adjacent conductors of the coil ($\varphi = \pi$).

Figure 3 shows the variation of the directivity as function of the frequency, for two values of serpentine coil wires, for a surface wave ($\theta = \pi/2$) in aluminum. The maximum directivity is obtained for frequencies equal to odd multiples of the ratio $\nu/(2d)$, where ν is the acoustic wave velocity and d is the distance between the serpentine wires. We can notice that increasing the number of wires enhances the frequency resolution of the EMAT.

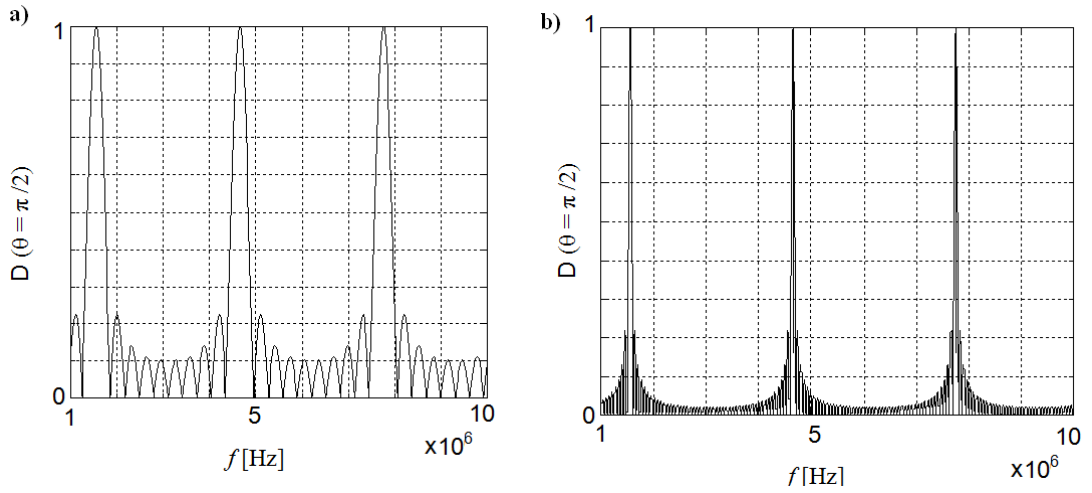


Fig. 3 – Variation of the directivity of a : (a) 10 wires and (b) 50 wires serpentine coil as function of the frequency, for a surface wave in aluminum material.

According to (6) the electric phase difference between two adjacent conductors is another way to control the orientation of the acoustic wave. For example, a wave at normal incidence ($\theta = 0$) is obtained for a phase shift ($\varphi = 0$), which corresponds to the configuration of the double spiral coil shown in Fig. 2-b. However, to apply any phase shift, each conductor must be supplied separately which may increase the complexity of the EMAT structure.

In the reception mode, the open circuit voltage induced in a serpentine coil is given as function of the directivity as follows [7] :

$$V_{\infty} = N L B D(\theta) v_t \sin c \left(\omega \frac{g \sin \theta}{2v} \right) e^{-\omega \frac{W \sin \theta}{v}} \quad (7)$$

In 7, is the angular frequency, B is the magnitude of the magnetic flux density, v and ν_t are respectively the acoustic wave speeds in the directions θ and $\theta = \pi/2$ (tangent to the surface of tested material), N and L are respectively the serpentine wires number and length, W is the serpentine coil width and g is the gap between the serpentine coil and

the tested material surface (Fig. 1).

For a given frequency, using a serpentine inductor, the acoustic beam can also be focused on a point (P) by varying the distance (d) between the wires (Fig. 4), according to the following relation [11] :

$$\sin \theta_i = \frac{v}{2d_i f} \tag{8}$$

In a fixed coordinate system (R, θ), as shown in Fig. 4, the relation (8) can be written as follows [11] :

$$\sin \theta_i = \frac{|R \sin \theta - x_i - d_i/2|}{\sqrt{(R \cos \theta)^2 + (R \sin \theta - x_i - d_i/2)^2}} \tag{9}$$

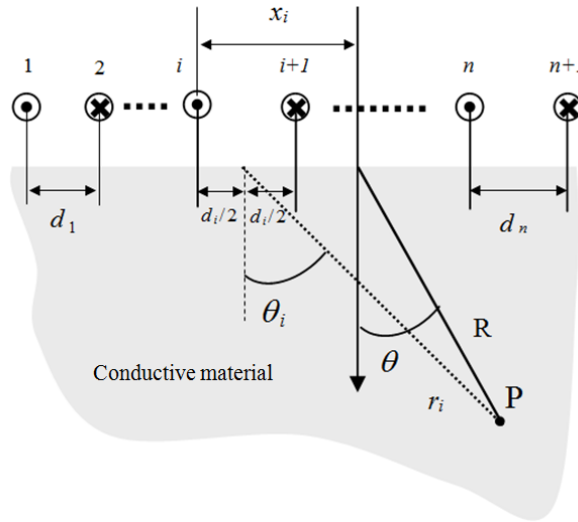


Fig. 4 – Acoustic beam focusing.

4. The transfer impedance

The transfer impedance Z characterizes the sensitivity of an EMAT [3]. The performance of an EMAT is conditioned by its transfer impedance; the latter has to be feeble in the emission mode and of important value in the reception mode.

As given in (10), it is the ratio between the induced voltage (V) by an acoustic wave and the electrical current (I) that has generated the latter. The transfer impedance accounts for all the factors that affect the electromagnetic acoustic transduction. It can be expressed as the product of the intrinsic impedance of the EMAT (Z_i) with a function F that represents the extrinsic factors that influence the transduction.

$$Z = FZ_i = VI^{-1} \tag{10}$$

The intrinsic transfer impedance is given by (11), where Z_A is the acoustic wave im-

pedance, B is the magnitude of the magnetostatic flux density, N is the number of wires (or turns) of the HF coil and S is the surface of the latter [3].

$$Z_i = B^2 N^2 S Z_A^{-1} \tag{11}$$

If different elements are used for the emission and reception, the intrinsic impedance is given by (11-1), where the subscripts E and R are related respectively the emission and reception elements.

$$Z_i = B_E B_R N_E N_R (S_E S_R)^{1/2} Z_A^{-1} \tag{12}$$

The most influent parameter is the gap (g) between the EMAT and the surface of the material. It has an influence on the eddy currents and on the magnetic flux density distribution in the material. This influence can be expressed as follows [3] :

$$F_g \approx \left(1 - \frac{2g}{X}\right) e^{-\frac{2\pi g}{Y}}$$

The relation 12 is only valid for $g \leq 0.1X$, where the parameter X represents the width of the magnetic circuit : $X = G$ for the structure presented in Fig. 1-a, and $X = DM$ for the structure presented in Fig. 1-b. The parameter Y represents the width of the HF coil periodicity : $Y = Rs$ for the single spiral coil (Fig. 2-a), $Y = W$ for the double spiral coil (Fig. 2-b) and $Y = 2d$ for the serpentine coil (Fig. 2-c).

5. Numerical modeling of EMATs

The modeling using global quantities as presented above is useful for EMATs pre-design but it is insufficient for the optimization and the evaluation of the interaction with the tested material. In this case, modeling using local quantities is necessary [9-13].

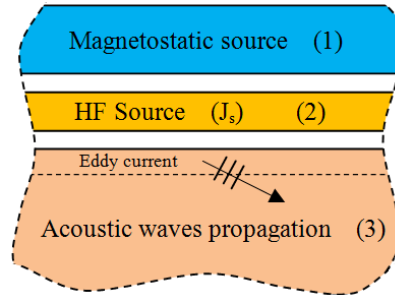


Fig. 5 – EMAT-tested sample system.

As presented in Fig. 5, an EMAT-sample system is constituted of a magnetostatic source region (1), a HF magnetic source region (2), and a conductive sample subject to eddy currents and acoustic wave propagation (3). All these active regions are separated by air which is, in this case, an inactive region for both the electromagnetic and acoustic quantities.

The coupled electromagnetic acoustic problem can be expressed as follows :

$$D(\vec{A}) = \vec{J} + \vec{J}_s \tag{13}$$

$$W(\vec{u}) = \vec{J} \times \vec{B} + \vec{F}_m \tag{14}$$

$$\vec{J} = (\sigma + \varepsilon \partial_t) \left(\partial_t \vec{A} + \vec{\nabla} V \right) + \sigma \vec{B} \times \partial_t \vec{u} \tag{15}$$

In 13, 14 and 15, D and W are functionals involving time and space simple and double derivatives, A and V are respectively the magnetic vector and electric scalar potentials, B is the magnetostatic flux density, σ is the electrical conductivity, ε is the electrical permittivity, J_s is a source current density, u is the displacement vector, ∂t denotes a time derivative and F_m represents magnetic forces [14].

Analytical and numerical methods based on finite element (FEM) and finite difference (FD) in time and frequency domains are commonly used to solve the coupled problem. However, if these methods generally converge, the spatio-temporal modeling may be considerably time consuming, unless making some assumptions and simplifications.

For the used frequencies, the displacement currents (i.e. the term $\varepsilon \partial t$.) can be neglected. In many problems, 2D modeling may be sufficient ; in this case, the electric scalar potential is not necessary, since the problem of the electrical current conservation does not arise. To avoid a coupling with the circuit equation in the HF source, which may lead to a high mesh density, it is suitable to impose a current source density (J_s) in this region. The magnetostatic and HF sources regions can thus be modeled using volume integral equations, avoiding the discretization of the air region [22]. As, for the used frequencies, the skin depth region is generally very thin, the surface impedance method could be very effective to evaluate the eddy currents [7]. For the acoustic part, the use of the dyadic Green's functions, when possible, is an interesting alternative, limiting the discretization to the source and the scattering regions [23-24].

6. Conclusion

EMATs were granted little interest for years due to their relatively low signal to noise ratio compared to classical acoustic transducers. However, the advances achieved in electronics and signal processing make them interesting alternatives for material control and characterization, and even for energy transfer and data communication. They arouse growing interest among the scientific community. In this context, this paper gives short notes which may be useful for EMATs design and modeling.

REFERENCES

- [1] P.A. Petcher, M.D.G. Potter and S. Dixon “A new electromagnetic acoustic transducer (EMAT) design for operation on rail”, *NDT & E International*, Volume 65, 1-7, July 2014.
- [2] Songling Huang, Zheng Wei, Wei Zhao and Shen Wang, “A New Omni-Directional

- EMAT for Ultrasonic Lamb Wave Tomography Imaging of Metallic Plate Defects”, *Sensors*, 14, 3458-3476, 2014.
- [3] B. W. Maxfield, A. Kuramoto, and J. K. Hulbert, “Evaluating EMAT Designs for Selected Applications”, *The Official Journal of the American Society for Nondestructive Testing*, 1166-1183, October 1987.
- [4] S. Aliouane, M. Hassam, A. Badidi Bouda and A. Benchaala, “ Electromagnetic Acoustic Transducers (EMATs) Design - Evaluation of their Performances”, 15th World Conference on Non-Destructive Testing, Rome, 15-21 October 2000.
- [5] B. Igarashi, G. A. Alers, and P. T. Purtscher, “Magnetostrictive EMAT efficiency as a materials characterization tool”, *Review of Progress in Quantitative Nondestructive Evaluation*. Vol. 17, 1485-1492, 1998.
- [6] G. A. Alers and L. R. Burns, “EMAT Designs for Special Applications”, *The Official Journal of the American Society for Nondestructive Testing*, 1184-1189, October 1987.
- [7] A.V. Clark, S.R. Schaps, and C.M. Fortunko, “A well-shielded EMAT for on line ultrasonic monitoring for GMA welding”, *IEEE ultrasonics symposium*, 337-340, 1991.
- [8] Hirotsugo Ogi, Masahiko Hirao and Toshihiro Ohtani, “Line focusing electromagnetic acoustic transducers for the detection of slit defects ”, *IEEE transactions on electronics, ferroelectrics and frequency control*, vol.46, n°2, 341-346, march 1999.
- [9] Dhayalan, R., Kumar, Anish, Rao, B. Purna Chandra, Jayakumar, T. “A hybrid finite element model for spiral coil electromagnetic acoustic transducer (EMAT)”, *International Journal of Applied Electromagnetics and Mechanics*, vol. 46, no. 3, 491-500, 2014.
- [10] Ludwig, Reinhold, Dai, X. W. “Numerical Simulation of Electromagnetic Acoustic Transducer in the Time Domain”, *Journal of Applied Physics*, 69(1), 89-98, 1991.
- [11] R. Lerch, M. Kaltenbacher, H. Landes, M. Hofer, J. Hoffelner, M. Raush, M. Schienner, “Advanced computer modelling of magnetomechanical transducers and their sound field”, *IEEE ultrasonics symposium*, 747-758, 2000.
- [12] R. Ludwing, Z. You and R. Palanisamy, “Numerical simulation of an electromagnetic acoustic transducer-receiver system for NDT application”, *IEEE transactions on magnetics*, vol.29, n°3, 2081-2088, may 1993.
- [13] Prashant Saxena, “On the general governing equations of electromagnetic acoustic transducers”, *Archive of Mechanical Engineering*, vol. 40, issue 2, 231-246, 2013.
- [14] Remo Ribichini, “Modeling of electromagnetic acoustic transducers”, PHD dissertation, Department of Mechanical Engineering Imperial College London, 2011.
- [15] R. Murayama, K. Fujisawa, H. Fukuoka, M. Hirao, S. Yonehara, “Nondestructive evaluation of material properties with EMAT”, *IEEE ultrasonics symposium*, 1159-1162, 1989.
- [16] B. Igarashi, G.A. Albert and P.T. Purtscher, “An ultrasonic measurement of magnetostriction”, *IEEE ultrasonics symposium*, Pages 709-712, 1997.
- [17] H. Ogi, M. Hirao and T. Ohtani, “Flow detection by line focussing electromagnetic acoustic transducers”, *IEEE ultrasonics symposium*, 653-656, 1997.
- [18] Tetsuya Uchimotoa, Toshiyuki Takagia, Toshiaki Ichiharaa, Gerd Dobmannb, “Evaluation of fatigue cracks by an angle beam EMAT–ET dual probe”, *NDT & E International*, Volume 72, 10-16, June 2015.
- [19] P.A.Petcher, S.Dixon, “Weld defect detection using PPM EMAT generated shear ho-

- horizontal ultrasound”, NDT&E International, Volume 74, 58-65, September 2015.
- [20] Riichi Murayama, Masayuki Kobayashi, Kenshi Matsumoto, Makiko Kobayashi, “Ultrasonic Inspection System Using a Long Waveguide with an Acoustic Horn for High-Temperature Structure” *Journal of Sensor Technology*, Volume 4, 177-185, 2014.
- [21] David J. Graham, “Investigation of methods for data communication and power delivery through metals”, PHD dissertation, School of Electrical, Electronic and Computer Engineering, Newcastle University, 2011.
- [22] Hocine Menana, Mouloud Féliachi, “An Integro-Differential model for 3D Eddy Current Computation in CFRPs”, *IEEE Transactions on Magnetics*, Vol. 47, NO. 4, 756 – 763, April 2011.
- [23] Ganquan Xie, Jianhua Li, and Feng Xie, “GL Acoustic Mechanical and EM Uniform Coupled Modeling and Inversion”, *PIERS Proceedings*, Cambridge, USA, 52-59, July 2-6, 2008.
- [24] N. P. Asimakis, I. S. Karanasiou, P. K. Gkonis and N. K. Uzunoglu, “ Theoretical analysis of a passive acoustic brain monitoring system”, *Progress In Electromagnetics Research B*, Vol. 23, 165-180, 2010.